Nuclear Engineering and Technology 53 (2021) 1587–1592

Contents lists available at ScienceDirect

Nuclear Engineering and Technology

journal homepage: www.elsevier.com/locate/net

Original Article

The evolution of radiation-induced point defects near symmetrical tilt Σ5 (310) <001> grain boundary in pure δ-plutonium: A molecular dynamics study

Yangzhong Wang [a], Wenbo Liu [a, *], Jiahui Zhang [a], Di Yun [a], Piheng Chen [b, **]

[a] Department of Nuclear Science and Technology, Xi'an Jiaotong University, Xi'an, 710049, China
[b] Institute of Materials, China Academy of Engineering Physics, Jiangyou, 621907, China

ARTICLE INFO

Article history:
Received 5 March 2020
Received in revised form
24 September 2020
Accepted 1 November 2020
Available online 4 November 2020

Keywords:
Radiation
Grain boundary
Point defects
Pure δ-plutonium
Molecular dynamics

ABSTRACT

The effects of the symmetrical tilt Σ5 (310) ⟨001⟩ grain boundary (GB) on the evolution of radiation-induced point defects in pure δ-plutonium (Pu) were studied by Molecular dynamics (MD) simulations. The evolution of radiation-induced point defects was obtained when primary knock-on atom (PKA) was respectively set as −15 Å and 15 Å far from the GB and the number of residual defects was obtained as the distance from PKA to GB was changed. According to the results, compared with vacancies, interstitial atoms were more easily absorbed by GB. In addition, the formation energy of point defects was also calculated. The results showed that there was almost no difference for the formation energy of vacancies in the all matrix. However, the formation energy of interstitial atoms close to the GB was lower than that in the other bulk regions.

1. Introduction

As a fissile material, Pu takes over a vital position in nuclear weapons and nuclear reactor fuels [1,2]. However, Pu can undergo α-decay, which forms helium atoms (5 MeV) and uranium nuclei (85.5 keV) [2,3]. These atoms with kinetic energy destroy the completed lattices, which induces a large number of point defects and forms plenty of defect structures, such as, dislocations and helium bubbles, which have a negative influence on the properties of materials [4–7]. In addition, there are six solid phases for pure Pu under normal pressure, which brings great difficulties and challenges to the researches [8–10]. Since the excellently ductile and malleable, the face-centered-cubic (FCC) structured δ-Pu is paid much attention to during the past decades [11,12]. However, δ-phase pure Pu is an unstable structure and turns into α-phase under the room temperature [11,13]. As a result, the elevated temperature of the material, for example 600 K, is needed to make the structure of δ-Pu stable [6,11,14].

It is accepted that GBs are usually act as sinks of point defects (self-interstitial atoms and vacancies) during radiation [15,16]. Void-denuded zones near GBs and incoherent twin boundaries were observed in copper (Cu) [17,18] and nickel (Ni) [19], while radiation-induced cavities were also observed predominantly along GBs in nanostructured Cu but less in the grain interior [20]. The simulation results also showed that GBs could be used as defect sinks to absorb interstitial atoms, which seriously affected the properties of materials [21–23]. Transmission electron microscopy (TEM) observations of Pu and its alloys after self-irradiation showed that bubbles preferred to form along GBs in 16-year-old and 42-year-old naturally aged materials [24,25]. Thus, it is necessary to understand the behaviors of radiation-produced point defects near GBs in polycrystalline Pu.

In the past decades, molecular dynamics (MD) simulations were successfully applied to simulate radiation-induced microstructure evolution in nuclear materials [12,13,26,27] and some researches had been carried out on pure Pu [12,13,28–30]. Robinson et al. [13] studied the number of point defects in δ-phase Pu when primary knock-on atom (PKA) energy varied from 0.4 to 10 keV, and they found that the number of defects was associated with the direction of PKA and sub-cascade at the higher energy of PKA. The interactions between GBs and defects were also discussed by Ao et al. [30], whose results showed that interstitial Pu atoms and

* Corresponding author.
** Corresponding author.
E-mail addresses: liuwenbo@xjtu.edu.cn (W. Liu), chenph@live.cn (P. Chen).

https://doi.org/10.1016/j.net.2020.11.001

interstitial helium atoms were prone to be absorbed than vacancies by GBs and helium bubbles were eventually shaped for these interstitial He atoms gathering together. However, there is still a lack of understanding the interactions of radiation-induced point defects and GBs without helium.

In the present work, the behaviors of radiation-induced point defects near the symmetrical tilt Σ5 (310) ⟨001⟩ GB in δ-Pu were investigated by using MD simulations. The structure of the paper was as follows. The methods and parameters such as the energy and direction of PKA were introduced in Section 2. The contents of Section 3 were the results of simulations, including the formation energy of point defect, the evolution of radiation defects and the relationship between distances from PKA to GB and defects yield. Section 4 was to summarize this research.

2. Methodology

The MD simulations were implemented by the Large-scale Atomic/Molecular Massively Parallel Simulator (LAMMPS) code in our work [31]. In the present work, the modified embedded atom method (MEAM), which could reproduce the properties and complicated behaviors of some materials or elements with relative accuracy, was utilized to describe the atomic interaction in Pu [32–34]. The Ziegler–Biersack–Littmark (ZBL) potential was also employed to model the close rang interactions simultaneously [35]. The parameters of MEAM potential used in the present work were as the same as those used in the work of Karavaev et al. [36], and the parameters of ZBL potential used in the present work were as the same as those used in the work of Robinson et al. [11].

The symmetric tilt Σ5 (310) ⟨001⟩ GB was built by creating two separate crystals with specific crystallographic orientations and connecting them along a plane normal [37]. In the newly created GB, there were some atoms distributed closer, which resulted in higher potential energy and thus needed to be deleted. Moreover, the conjugate gradient algorithm was applied to implement the energy minimization in the system and the energy tolerance was set as 10^{-12} eV.

The schematic diagram of the simulation structure with Σ5 (310) ⟨001⟩ GB was shown in Fig. 1. A cubical simulation box with about 150, 000 atoms was first thermalized for 20 ps at 600 K and Nose-Hoover thermostat and barostat were used to control the temperature and pressure of the system. After that, the outer region of the box was set as the thermostat region to control temperature

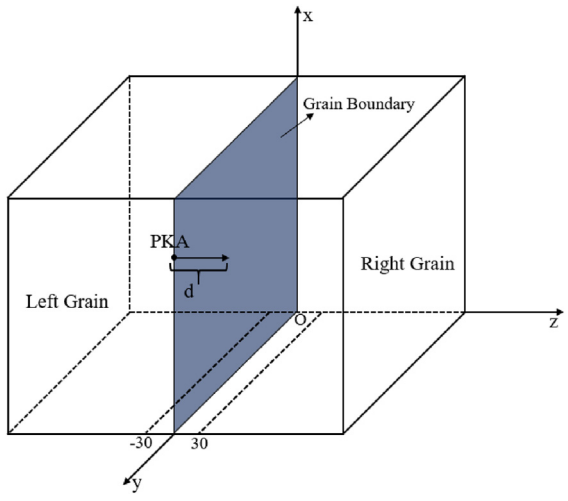

Fig. 1. Sketch of the simulation box used in the study.

during simulations and the inner region was controlled by micro-canonical ensemble. PKA with a kinetic energy of 2 keV in [001] direction was introduced to generate the radiation damage. The entire simulations lasted for 100 ps and could be discerned into three stages. In the initial stage, the timestep was set 0.02 fs to accurately simulate the collision cascades. The next stage corresponded to the recombination of point defects and the timestep was 0.1 fs. In the final stage, the system evolved slowly and point defects might diffuse in a longer time scale, so the timestep was set 1.0 fs. Furthermore, periodic boundary condition was applied to three orientations and ten simulations were carried out for each condition to reduce random errors.

Open Visualization Tool (OVITO), which was developed by Stukovski [38], was used in the present work to perform visualization and data analysis, and Wigner-Seitz method was used to confirm and count interstitial atoms and vacancies [28]. In the Wigner-Seitz method, a reference configuration before PKA introduced was usually required, and a displaced configuration with existed damages could be analyzed. In the present work, every atom was defined as its space region in the reference configuration by the Wigner-Seitz analysis algorithm. There were some sites in the displaced configurations occupied by no atoms, which were defined as vacancies. In other wise, if some sites in the displaced configurations were occupied by more than one atom, then they could be named as interstitial atoms. It should be noted that the region close to the GB (5.03 Å in both sides from the GB) was not taken into account for studying the effect of GB on the progress of radiation-induced defects when counting the number of defects in the study.

3. Results and discussion

3.1. Defect formation energy in pure δ-Pu

It was necessary to calculate the formation energy of vacancies and interstitial atoms for understanding the interactions of radiation-induced point defects and GB. The method adopted in the present work was an analogy with that in other elements, for example, Cu [39] or Zirconium (Zr) [40]. The formation energy of point defects is calculated following the equations [41]:

$$E_{int} = E_{aft} - E_{pri} - E_{coh} \tag{1}$$

and:

$$E_{vac} = E_{aft} - E_{pri} + E_{coh} \tag{2}$$

where E_{int} was the formation energy of interstitial atom and E_{vac} corresponded to the formation energy of vacancy, E_{aft} (E_{pri}) represented the total potential energy of the system with (without) a point defect and E_{coh} was the cohesive energy per Pu atom of a FCC lattice.

The formation energy of interstitials and vacancies in pure δ-Pu as a function of distance to GB was illustrated in Fig. 2. It could be found that the formation energy of vacancies was lower than that of interstitial atoms in the whole simulated region. However, there was no significant difference for the formation energy of vacancies in the whole bulk. Moreover, although smaller than the DFT results [42,43], the calculation result of the formation energy of vacancies was similar with the results calculated by other people [13,29] though MD with MEAM. However, the formation energy of interstitial atoms in a certain width was lower than that in other part of the matrix, which facilitated the accumulation of interstitial atoms near GB, and the width was considered to be the width of GB. Hence, the width of symmetric tilt Σ5 (310) ⟨001⟩ GB in δ-Pu was

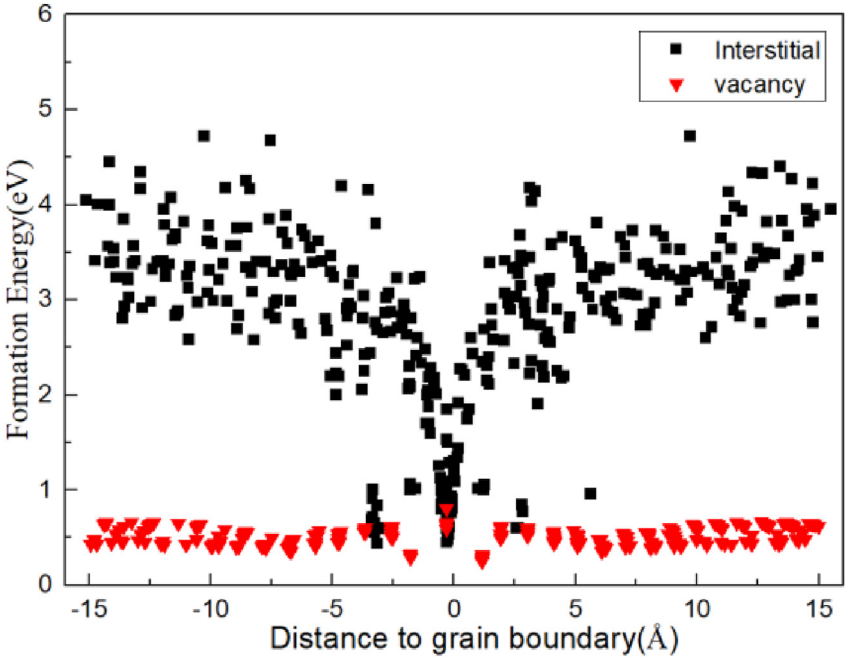

Fig. 2. Formation energy of interstitial atoms and vacancies in pure Pu as a function of distance to GB.

estimated as ~10.06 Å after the calculated results shown in Fig. 2 were carefully analyzed. The analogous situation also appeared in the simulation of other material [21,23,44]. In other words, compared with vacancies, interstitial atoms were prone to be absorbed by symmetric tilt Σ5 (310) ⟨001⟩ GB in δ-Pu from the perspective of formation energy when the entire system was in a thermodynamically stable state.

3.2. The evolution of radiation defects

The whole defects evolution as a function of time was shown in Fig. 3. It could be seen in both of the figures that, the number of point defects increased dramatically and reached its maximum value at about 0.8 ps in the initial stage, which meant that there were plenty of atoms left the lattice sites after the introduction of PKA. Subsequently, interstitial atoms and vacancies quickly recombined and the amount of point defects rapidly reduced. Finally, during the annealing process, the defects tardily recombined and vanished. The majority of interstitial atoms and vacancies recombined and disappeared and only a small part of defects would remain in the bulk. When PKA was seated at 15 Å and the initial direction of PKA was along the [001] direction (Fig. 3a), collision cascades and GB almost did not coincide. Hence, the radiation-produced microstructures could be considered as the same collision cascades caused in single crystal. However, when PKA was seated at −15 Å and the initial direction of PKA was still along the [001] direction (Fig. 3b), GB had a serious influence on the evolution of collision cascades. As a result, there were fewer point defects yielded under the circumstance (Fig. 3b), compared with that after radiation when PKA was seated at 15 Å (Fig. 3a).

At the same time, the ratio of the number of vacancies to the number of interstitial atoms over time when PKA was set as −15 Å was displayed in Fig. 4, which was basically more than 1 and was less than 1 only in local cases during the entire simulation period. In addition, the changes of the ratio over time, obviously, were non-monotonic. In the first stage, when the collisions occurred

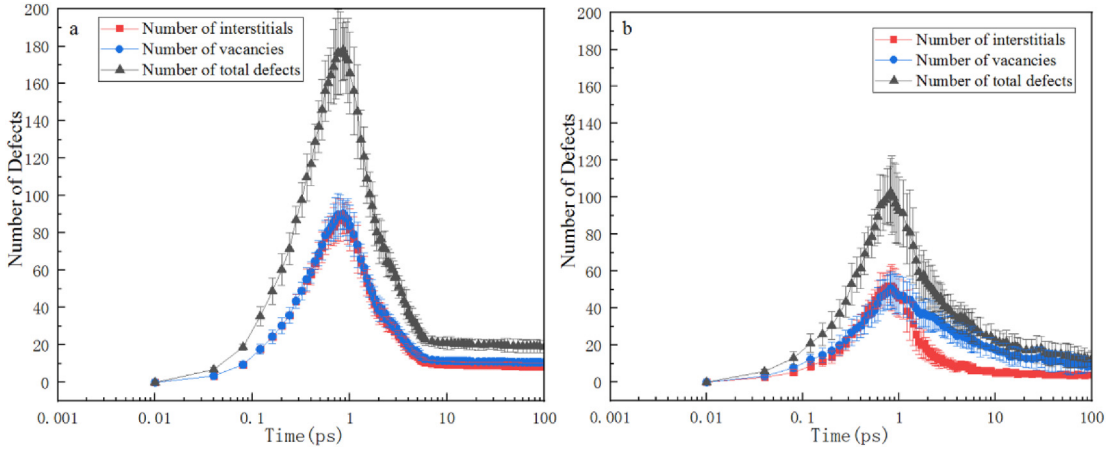

Fig. 3. Comparison of the whole evolution of number of interstitial atoms, vacancies and total defects with time: (a) PKA was located at 15 Å, (b) PKA was located at −15 Å

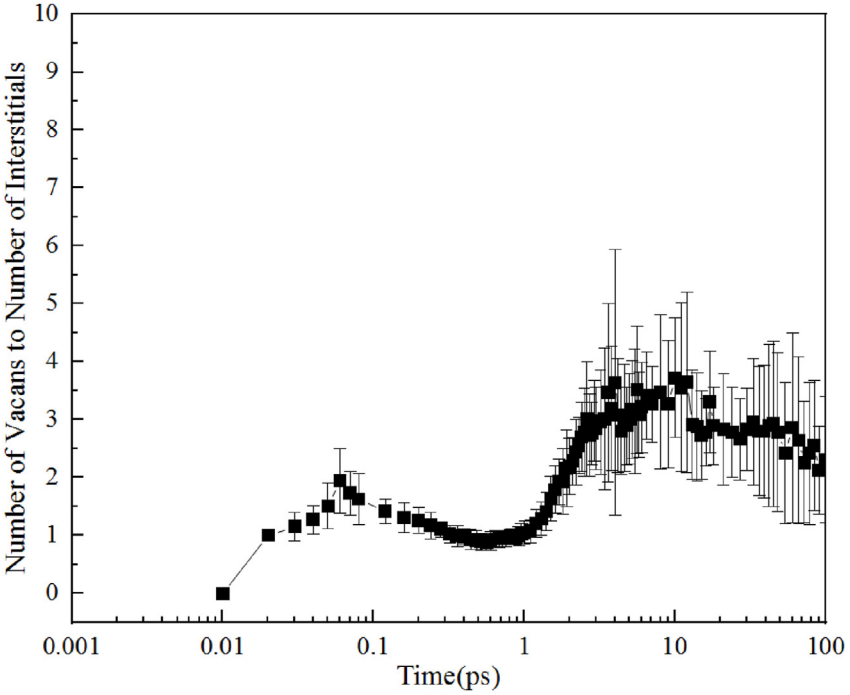

Fig. 4. Ratio of the number of vacancies to the number of interstitial atoms over time.

rapidly, there were some interstitial atoms first reaching the range affected by GB and more vacancies were located at other areas. In this case, the ratio tended to increase. When the collisions took place in the region influenced by GB, there were some atoms in the GB leaving the areas affected by GB and vacancies in the influence range of the GB increased, which corresponded to a decline of the ratio in the second stage. The next stage was that point defects begun to recombine and disappear and there were some interstitial atoms absorbed by GB, which leaded to a gradual increase of the ratio. In the last stage, some interstitial atoms released by GB combined with vacancies, which meant that the ratio of the number of vacancies to the number of interstitial atoms showed a downward trend. The phenomenon was also similar with the simulation of Cu by Bai et al. [23] and the reason for the appearance was that there existed some vacancies near GB, which facilitated the migration of interstitial atoms in the GB. However, because of the small number of point defects generated, the error of ratio was a little large, and fluctuated frequently during the slow recombination of point defects.

In order to further investigate the entire process of collisions, some snapshots of the point defects distributions during simulations were shown in Fig. 5. It could be seen in all the figures that, the vacancies distributed in the inner region of collision, while the interstitial atoms spread in a wider region. The reason for the formation of the "core-shell" structure could be attributed to the difference of the migration energy between vacancy and interstitial

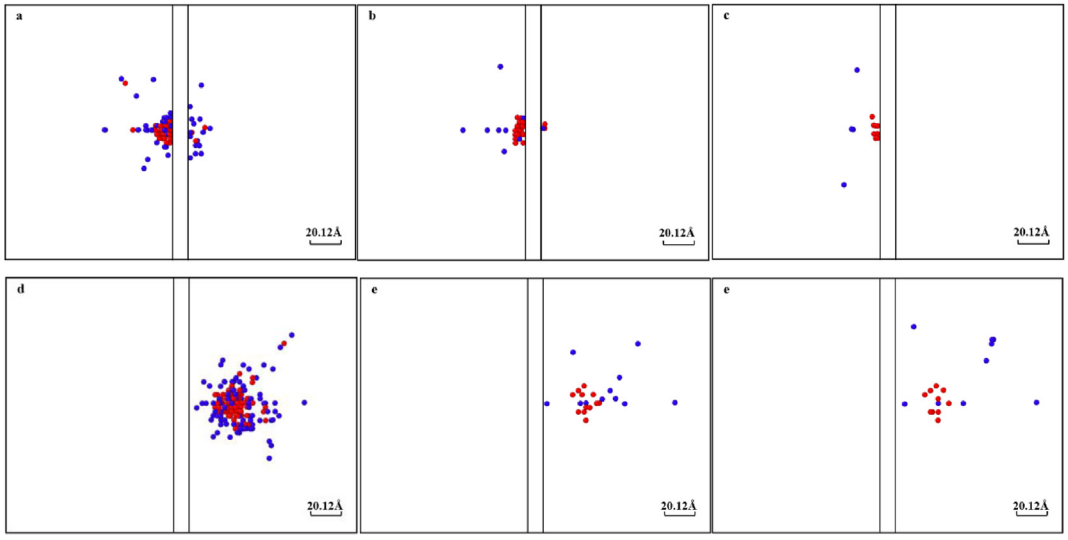

Fig. 5. Snapshots of defects distributions of PKA set as −15 Å at (a) 0.8 ps, (b) 5.0 ps, (c) 100.0 ps and 15 Å at (d) 0.8 ps, (e) 5.0 ps, (f)100.0 ps. Blue atoms are interstitial atoms, and red atoms are vacancies. (For interpretation of the references to colour in this figure legend, the reader is referred to the Web version of this article.)

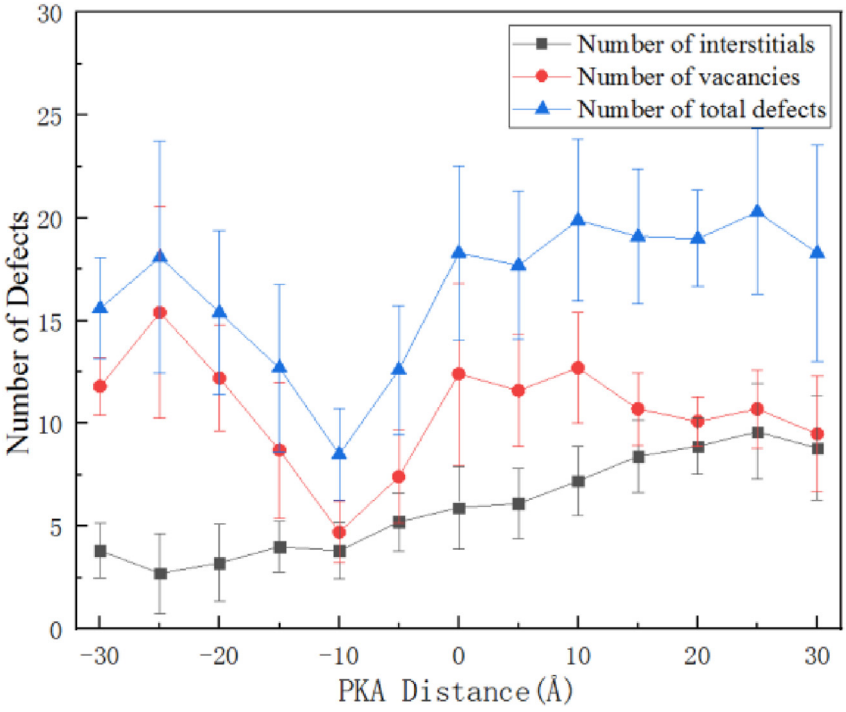

Fig. 6. Number of residual interstitial atoms, vacancies and total defects as a function of distance from PKA to the GB.

atom at the same temperature. In addition, it was easy to notice that the core of the collision cascades was close to the GB when PKA was set as −15 Å (Fig. 5a). The number of vacancies was larger than that of interstitial atoms, and the majority of the vacancies were closer to the GB than the interstitial atoms (Fig. 5b and 5c). That was to say, it was interstitial atoms that were more likely to be assimilated by the GB. The phenomenon had been also found in the research of other mental materials [15,21,41,45]. However, as demonstrated in Fig. 5d, the collision cascades mainly occurred on the right side of the GB and almost unaffected by the GB when PKA was set as 15 Å. At the same time, it could be found from Fig. 5e and 5f, there was almost no difference between the number of interstitial atoms and the number of vacancies.

3.3. The dependence of PKA distance to GB on defects production

The variation of radiation-induced residual defects as a function of the distance from PKA to GB was plotted in Fig. 6. The distance of PKA to GB was −30 Å at the beginning and varied from −30 Å to 30 Å, 5 Å per change. The initial velocity direction of PKA was perpendicular to the GB. It was easy to find from Fig. 6 that the number of point defects reached a minimum when PKA was set as −10 Å, since the core of the collision cascades almost coincided with GB in this situation. In other words, GB had a serious effect on the evolution of radiation-induced point defects. Before PKA was located at −10 Å, as the distance from PKA to GB increased by degrees, the effect of GB on the evolution of point defects gradually weakened and the total number of residual defects gradually increased. At the same time, the disparity between the number of residual interstitial atoms and the number of residual vacancies was gradually increasing, since the number of vacancies increases gradually, which promoted the recombination of interstitial atoms and vacancies, and interstitial atoms were assimilated by GB. Though, when PKA was set on the right side of GB, PKA couldn't pass directly through GB. There were some scattered atoms colliding with atoms in GB unless the distance between PKA and GB was far enough, since the scattering direction of atomic collisions was random when atoms collided with each other. So even after PKA was set as 5 Å, some interstitial atoms could be still absorbed by GB, which leaded to the consequence that the number of surviving vacancies was more than that of surviving interstitial atoms. But with the distance from PKA to the GB gradually increasing, the influence of GB gradually weakened and the number of residual vacancies and the number of residual interstitial atoms gradually approached, which was shown in Fig. 6. The whole evolution of irradiation damage simulations was gradually close to that of single crystal.

4. Conclusions

We had investigated the effects of Σ5 (310) ⟨001⟩ GB on the evolution of radiation-induced point defects at different distances from PKA to the GB and the formation energy of point defects by MD simulations.

According to the calculation results of the formation energy, the formation energy of interstitial atoms affected by the GB was a little smaller than that of interstitial atoms unaffected by the GB, but the formation energy of interstitial atoms was greater than the formation energy of vacancies as a whole. Consequently, the width of symmetric tilt Σ5 (310) ⟨001⟩ GB could be regarded as ~10.06 Å according to the change of the formation energy of interstitial atoms. The formation energy of vacancies was hardly affected by the GB. Moreover, the evolution of radiation-induced point defects when PKA was located at 15 Å and −15 Å respectively showed that, compared with vacancies, interstitial atoms were prone to be absorbed by GB. However, it could be known that some interstitial atoms were also emitted from GB and recombined with vacancies in the recombination process by investigating the evolution of radiation-induced point defects.

The results also revealed that the number and distribution of radiation-induced point defects were significantly influenced by the distance between PKA and the GB. As the distance from PKA to

the GB changed from −30 Å to 30 Å, it could be found that the number of residual point defect reached their minimum for the process of collision cascades terribly influenced by GB when PKA was located at −10 Å. When the distance between GB and PKA was far enough, there was almost no difference between the number of interstitial atoms and the number of vacancies, since GB had a faint influence on the evolution of point defects.

Declaration of competing interest

The authors declare that they have no known competing financial interests or personal relationships that could have appeared to influence the work reported in this paper.

Acknowledgements

Financial support provided by the NSAF Joint Fund (No. U1830124), National Natural Science Foundation of China (No. 11705137, 11675126) and China Postdoctoral Science Foundation (No. 2019M663738) is acknowledged.

References

[1] G.S. Chang, J. Alloys Compd. 444–445 (2007) 434–437.
[2] F.C. Wu, P. Wang, X.Y. Liu, H.A. Wu, J. Nucl. Mater. 484 (2017) 7–15.
[3] L. Berlu, G. Jomard, G. Rosa, P. Faure, J. Nucl. Mater. 374 (2008) 344–353.
[4] M. Robinson, S.D. Kenny, R. Smith, M. Storr, J. Nucl. Mater. 423 (2012) 16–21.
[5] V.V. Dremov, A.V. Karavaev, S.I. Samarin, F.A. Sapozhnikov, M.A. Zocher, D.L. Preston, J. Nucl. Mater. 385 (2009) 79–82.
[6] S.M. Valone, M.I. Baskes, R.L. Martin, Phys. Rev. B 73 (2006) 214209.
[7] B.Y. Ao, P.H. Chen, P. Shi, X.L. Wang, W.Y. Hu, L. Wang, Commun. Comput. Phys. 11 (2012) 1205–1225.
[8] M.I. Baskes, A.C. Lawson, S.M. Valone, Phys. Rev. B 72 (2005), 014129.
[9] V.V. Dremov, A.V. Karavaev, F.A. Sapozhnikov, M.A. Vorobyova, D.L. Preston, M.A. Zocher, J. Nucl. Mater. 414 (2011) 471–478.
[10] B.Y. Ao, X.L. Wang, P.H. Chen, P. Shi, W.Y. Hu, J.Y. Yang, Acta Phys. Sin. 59 (2010) 422–429.
[11] M. Robinson, S.D. Kenny, R. Smith, M.T. Storr, Nucl. Instrum. Methods Phys. Res. Sect. B Beam Interact. Mater. Atoms 269 (2011) 2539–2548.
[12] B.Y. Ao, X.L. Wang, W.Y. Hu, J.Y. Yang, J.X. Xia, J. Alloys Compd. 444–445 (2007) 300–304.
[13] M. Robinson, S.D. Kenny, R. Smith, M.T. Storr, E. McGee, Nucl. Instrum. Methods Phys. Res. Sect. B Beam Interact. Mater. Atoms 267 (2009) 2967–2970.
[14] M.I. Baskes, S.Y. Hu, S.M. Valone, G.F. Wang, A.C. Lawson, J. Comput. Aided Mater. Des. 14 (2007) 379–388.
[15] D. Mo, J. Cai, Y.L. Li, Y.D. Wang, Mater. Sci. Forum 913 (2018) 642–649.
[16] F. Yazdandoost, R. Mirzaeifar, Comput. Mater. Sci. 131 (2017) 108–119.
[17] S.J. Zinkle, K. Farrell, J. Nucl. Mater. 168 (1989) 262–267.
[18] B.N. Singh, A. Horsewell, D.S. Gelles, F.A. Garner, J. Nucl. Mater. 191–194 (1992) 1172–1176.
[19] C.W. Chen, R.W. Buttry, Radiat. Eff. 56 (1981) 219–228.
[20] W.Z. Han, E.G. Fu, M.J. Demkowicz, Y.Q. Wang, A. Misra, J. Mater. Res. 28 (2013) 2763–2770.
[21] J.H. Zhang, W.B. Liu, P.H. Chen, H. He, C.H. He, D. Yun, Nucl. Instrum. Methods Phys. Res. Sect. B Beam Interact. Mater. Atoms 451 (2019) 99–103.
[22] D. Terentyev, X. He, A. Serra, J. Kuriplach, Comput. Mater. Sci. 49 (2010) 419–429.
[23] X.M. Bai, A.F. Voter, R.G. Hoagland, M. Nastasi, B.P. Uberuaga, Science 327 (2010) 1631–1634.
[24] T.G. Zocco, A.J. Schwartz, J. Occup. Med. 55 (2003) 24–27.
[25] A.J. Schwartz, M.A. Wall, T.G. Zocco, W.G. Wolfer, Phil. Mag. 85 (2005) 479–488.
[26] F.B. Li, G. Ran, N. Gao, S.Q. Zhao, N. Li, Chin. Phys. B 28 (2019), 085203.
[27] Z.Y. Liu, B. He, X. Qu, L.B. Niu, R.S. Li, F. Wang, Phys. Rev. B 28 (2019), 083401.
[28] A. Kubota, W.G. Wolfer, S.M. Valone, M.I. Baskes, J. Comput. Aided Mater. Des. 14 (2007) 367–378.
[29] G. Jomard, L. Berlu, G. Rosa, P. Faure, J. Nadal, N. Baclet, J. Alloys Compd. 444–445 (2007) 310–313.
[30] B.Y. Ao, J.X. Xia, P.H. Chen, W.Y. Hu, X.L. Wang, Chin. Phys. B 21 (2012), 026103.
[31] S. Plimpton, J. Comput. Phys. 117 (1995) 1–19.
[32] M.I. Baskes, Phys. Rev. B 46 (1992) 2727–2742.
[33] M.I. Baskes, Phys. Rev. B 62 (2000) 15532–15537.
[34] M.I. Baskes, K. Muralidharan, M. Stan, F.J. Cherne, J. Occup. Med. 55 (2003) 41–50.
[35] J.F. Ziegler, J.P. Biersack, Treatise on Heavy-Ion Science, 1985, pp. 93–129.
[36] A.V. Karavaev, V.V. Dremov, G.V. Ionov, J. Nucl. Mater. 496 (2017) 85–96.
[37] J.W. Cahn, Y. Mishin, A. Suzuki, Acta Mater. 54 (2006) 4953–4975.
[38] A. Stukowski, Model. Simulat. Mater. Sci. Eng. 18 (2009), 015012.
[39] A. Suzuki, Y. Mishin, Interface Sci. 11 (2003) 425–437.
[40] A. Arjhangmehr, S.A.H. Feghhi, Sci. Rep. 6 (2016) 23333.
[41] X.Y. Li, W. Liu, Y.C. Xu, C.S. Liu, Q.F. Fang, B.C. Pan, J.L. Chen, G.N. Luo, Z.G. Wang, Nucl. Fusion 53 (2013) 123014.
[42] S.C. Hernandez, F.J. Freibert, R.G. Hoagland, B.P. Uberuaga, J.M. Wills, Phys. Rev. 2 (2018), 085005.
[43] G. Robert, A. Pasturel, B. Siberchicot. Europhysics Letter 71 (2005) 412–417.
[44] X.M. Bai, L.J. Vernon, R.G. Hoagland, A.F. Voter, M. Nastasi, B.P. Uberuaga, Phys. Rev. B 85 (2012) 214103.
[45] M. Samaras, P.M. Derlet, H. Van Swygenhoven, M. Victoria, Phys. Rev. Lett. 88 (2002) 125505.